

## NEW CONTRIBUTIONS TO THE HYDROGEN EMBRITTLEMENT F.I.P. TEST IN AMMONIUM THIOCYANATE

J. Toribio\* and M. Elices\*

The Ammonium Thiocyanate Test (ATT) was proposed by FIP as a suitable method for checking the hydrogen embrittlement susceptibility of prestressing steels. The main disadvantage of this test is the scattering of the results.

In this work a great number of experimental results at different applied stresses is analyzed in four pearlitic eutectoid steels. A diffusion model, based on hydrogen concentration and hydrostatic stress gradients, is proposed. The residual stresses measured on the wire surface by X-ray diffraction are also considered in the model.

Times to rupture, as a function of applied stress, were obtained showing good agreement with experimental data, and illustrating the role of previous residual stress distribution in hydrogen embrittlement, and so the increasing scattering of the results when the externally applied stress is lower.

### INTRODUCTION

High strength steel wires (ultimate tensile strength > 1500 MPa), usually cold drawn eutectoid steels, are widely used for prestressing concrete structures. There is general agreement that hydrogen embrittlement plays an important role in the environmental cracking of such steels.

The Ammonium Thiocyanate Test (ATT) was proposed by FIP as a suitable method to determine the hydrogen embrittlement susceptibility of prestressing steels (1). In spite of some objections to this standard corrosion test proposed by Parkins et. al. (2), it is still the best suited to steel control and acceptance.

Therefore, any contribution to a better understanding of the meaning of the ATT, and specially of the influence of stress level on the time to rupture, should be welcome, both from the scientific point of view and for practical and economic reasons.

\* Department of Materials Science, Polytechnical University of Madrid. E.T.S. I. Caminos, Ciudad Universitaria, 28040 Madrid, Spain.

EXPERIMENTAL RESULTS

Four commercial prestressing steel wires were tested (3). All them were eutectoid cold drawn steels, produced by patenting 12 mm diameter rods in a molten lead bath to produce fine pearlite, after which the rods were cold drawn to achieve 7 mm diameter wires. Finally, the drawn wires were stress-relieved at 425°C for a few seconds and cooled in water (steels A, B and D) or in oil (steel C).

The results are shown in Fig. 1 for the four tested steels. For each stress level the average time to rupture and the interval corresponding to the standard derivation are plotted. Two considerations must be made:

- These tests present a high level of scattering in time to rupture, a variable which reflects susceptibility of the metal to hydrogen embrittlement.
- The scattering is non-uniform: for high stress levels is small, and clearly increases when the applied stress is lower.

The explanation should be sought in any variable able to modify the externally applied stress state. Internal residual stresses in the material have been proposed as the cause of these phenomena (4).

THEORETICAL MODELDiffusion

The theoretical hydrogen diffusion model is based on two main hypotheses:

D1) TRANSPORT: The main hydrogen transport mechanism is diffusion, neglecting therefore the transport by dislocation movement, according to previous research of the authors with this kind of steel (5,6).

D2) ABSORPTION: The absorption of adsorbed hydrogen at the surface is quasi-instantaneous, as is demonstrated in previous works (5,6).

The diffusion equations are modified Fick's Laws to include terms dependent on the hydrostatic stress (7,8):

$$\mathbf{J} = -D \mathbf{grad} c + Mc \mathbf{grad} \sigma \quad (1)$$

$$\frac{\partial c}{\partial t} = D \Delta c - M \mathbf{grad} c \cdot \mathbf{grad} \sigma - Mc \Delta \sigma \quad (2)$$

where  $\sigma$  is the hydrostatic stress ( $\sigma = \text{tr } \boldsymbol{\sigma} / 3$ ),  $D$  the diffusion coefficient and  $M$  a second coefficient dependent on the latter:

$$M = \frac{DV^*}{RT} \quad (3)$$

where  $V^*$  is the molar partial volume of hydrogen,  $R$  the ideal gases constant and  $T$  the absolute temperature.

The concentration of absorbed hydrogen in the boundary is, according to D2:

$$c_o^* = c_o \exp\left(\frac{V^*\sigma}{RT}\right) \quad (4)$$

Boltzmann's distribution where  $c_o$  is the equilibrium concentration without stresses, and  $\sigma$  the hydrostatic stress at the boundary.

The problem to solve is the one referring to a cylinder of radius  $a$  and  $c = c_o^*$  as the value of hydrogen concentration at the boundary ( $r = a$ , adopting  $r$  and  $z$  as the cylindrical coordinates). Taking into account the cylindrical symmetry, the diffusion equation leads to:

$$\frac{\partial c}{\partial t} = D \left( \frac{\partial^2 c}{\partial r^2} + \frac{1}{r} \frac{\partial c}{\partial r} \right) - \frac{DV^*}{RT} \frac{\partial c}{\partial r} \frac{\partial \sigma}{\partial r} - \frac{DV^*}{RT} c \left( \frac{\partial^2 \sigma}{\partial r^2} + \frac{1}{r} \frac{\partial \sigma}{\partial r} \right) \quad (5)$$

in the interval  $0 \leq r \leq a$ , with the initial condition:

$$c(r,0) = 0 \quad ; \quad 0 \leq r \leq a \quad (6)$$

and the boundary conditions:

$$\frac{\partial c}{\partial r}(0, t) = 0 \quad ; \quad t \geq 0 \quad (7)$$

$$c(a, t) = c_o^* \quad ; \quad t \geq 0 \quad (8)$$

In this research the influence of axial residual stress distribution in the cylinder is analyzed. To achieve this, six kinds of distribution are considered (see Fig.2, where  $x$  is the depth from the boundary of the cylinder). Since the critical crack depth is never higher than  $350 \mu\text{m}$ , only  $400 \mu\text{m}$  of residual stress distributions have been plotted. Outside this region, the equilibrium conditions are applied. Distribution 1 corresponds to the material without stresses. 2, 3, 4 and 5 are typical distributions measured in commercial wires. Distribution 6 models a rolling process on the wire, and allows a study of the benefits of such a technique, increasing the time to rupture.

Equation (5) with conditions (6), (7), and (8) does not have an analytical solution, and thus the Finite Element method for the stress-strain problem was used together with a Weighted Residuals formulation for the diffusion problem. The chosen discretization time interval was  $D \Delta t / a^2 = 0.01$ , following (8).

The discretization was checked by solving a specific problem with an analytical solution: the diffusion in a cylinder free of stresses. In this case, the equation (5) becomes:

$$\frac{\partial c}{\partial t} = D \left( \frac{\partial^2 c}{\partial r^2} + \frac{1}{r} \frac{\partial c}{\partial r} \right) \quad (9)$$

in the internal  $0 \leq r \leq a$ , with the initial condition (6) and the boundary conditions (7) and (8), the latter with value  $c_0$  as a particular case.

The solution is (9):

$$\frac{c}{c_0} = 1 - \frac{2}{a} \sum_{n=1}^{\infty} \frac{J_0(\alpha_n r)}{\alpha_n J_1(\alpha_n a)} \exp(-D \alpha_n^2 t) \quad (10)$$

where  $J_0$  and  $J_1$  are the Bessel functions with orders zero and one, respectively, and  $\alpha_n$  the positive roots of the equation  $J_0(\alpha_n a) = 0$ . The Bessel functions can be extended in series:

$$J_n(x) = \sum_{k=0}^{\infty} \frac{(-1)^k (x/2)^{n+2k}}{k! \Gamma(n+k+1)} \quad (11)$$

where  $\Gamma$  is the Euler gamma function, which for entire argument, as in the case of this problem, has the following expression:

$$\Gamma(p) = (p - 1)! \quad (12)$$

The analytical solution (exact) is compared in Fig.3 with the numerical one. The agreement is excellent, with errors lower than 4%.

### Fracture

The following hypotheses are adopted regarding fracture:

F1) INITIATION: Fracture initiates when the hydrogen reaches a critical concentration  $c_c$  over a distance  $x_c$  (damaged zone or critical size for initiation); then it is assumed that a crack with depth  $x_c$  is created.

F2) PROPAGATION: The propagation time, i.e., the time required to propagate the crack from the initial size  $x_c$  up to a critical value to produce the final rupture of the sample will be neglected. That is, it is assumed that the initiation time coincides with the time to rupture. Such assumption was proved experimentally by Piñero (10) with these steels.

With both hypotheses the solution of the problems requires the obtention of the time to rupture  $t_R$ , the point at which the hydrogen reaches a critical concentration  $c_c$  over a critical distance  $x_c$ . The fracture condition is based on the stress intensity factor:

$$K_I = K_{IHE} \quad (13)$$

where  $K_{IHE}$  is the threshold stress intensity factor for the hydrogen environment.

The expression for the stress intensity factor is, for this problem.

$$K_I = M (\sigma_{ap} + \sigma_{res}) \sqrt{\pi x} \quad (14)$$

in which  $M$  is a non-dimensional factor dependent on the geometry,  $\sigma_{ap}$  the applied stress and  $\sigma_{res}$  the residual stress prior to cracking. Equation (14) is only valid for uniform residual stress distribution, and those considered in Fig. 2 are not constant. However, they are considered uniform to calculate the stress intensity factor (the error is negligible), but not to study the diffusion.

The value  $M$  was calculated by Astiz (11):  $M = 0.94$ . The fracture condition is, thus:

$$0.94 (\sigma_{ap} + \sigma_{res}) \sqrt{\pi x_c} = K_{IHE} \quad (15)$$

#### LIFE PREDICTION

The final aim of this research is to determine the time to rupture of these steels in hydrogen environment. The following computation data were adopted:

$$V^* = 2 \text{ cm}^3 / \text{mol}$$

$$D = 4,99 \cdot 10^{-12} \text{ m}^2/\text{s} \quad (35^\circ\text{C})$$

$$c_c/c_0 = 1,24 \quad (35^\circ\text{C})$$

$$K_{IHE} = 0.27 K_{IC}$$

To obtain the curves for applied stress  $\sigma_{ap}$  vs. time to rupture  $t_R$  and compare them with the experimental results given in Fig.1, the procedure is the following: for each applied stress, the critical zone is obtained by means of:

$$x_c = \frac{1}{\pi} \left[ \frac{K_{IHE}}{0.94 (\sigma_{ap} + \sigma_{res})} \right]^2 \quad (16)$$

in which  $\sigma_{res}$  represents the residual stress value for the horizontal part of the curves given in Fig.2.

On the other hand, the non-dimensional critical concentration is, with respect to the boundary concentration:

$$\frac{c_c}{c_o^*} = \frac{c_c / c_o}{\exp [(\sigma_{ap} + \sigma_{res\ c}) V^* / RT]} \quad (17)$$

where  $\sigma_{res, c}$  is the residual stress at the boundary ( $r=a$ ), with value zero in all residual stress distributions except number 6.

The critical depth (6) and the critical concentration (17) are introduced in the diffusion results (concentration in all points of the sample for any time). First of all, the hydrogen concentration in the  $x_c$  depth point in any instant is calculated; later, the time for which such a concentration reaches the value  $c_c / c_o^*$  is obtained.

Fig.4 shows the results from the theoretical model (one line for each residual stress distribution) compared with the experimental results (shaded area). The agreement is excellent, because curve 1 - which corresponds to a material without residual stresses - exactly fits the central tendency, and curves 2, 3, 4 and 5 - which correspond to materials with residual stresses associated with the manufacturing process - cover the experimental band with very good agreement. Compressive residual stresses extend the life time of the wires, and tensile residual stresses decrease it. Curve 6 corresponds to a material which has suffered a rolling process after manufacture, introducing strong compressive residual stresses which clearly extend the life.

The shape of the curves calculated from the theoretical model explains the scattering of the FIP Test, increasing for lower applied stresses, since the slope of the curves is smaller for decreasing applied stress.

#### CONCLUSIONS

- 1) The influence of residual stresses on the hydrogen embrittlement of steels was theoretically modelled, obtaining a very accurate prediction of the experimental results.
- 2) The role of diffusion in the hydrogen transport in metals was confirmed.
- 3) The importance of the applied stress in the scattering of the results (higher for lower stresses), was pointed out.
- 4) The temperature of the test must be carefully controlled, because the results are strongly dependent on it, through the diffusion coefficient.
- 5) Rolling processes clearly extend the life of the wires, by introducing high compressive residual stresses.

REFERENCES

- (1) FIP-78. Stress Corrosion Test. Technical Report No.5 FIP, Wexham Springs. Slough U.K. 1981.
- (2) Parkins, R.N., Elices, M., Sánchez-Gálvez, V., "Some comments on the standardization of tests methods for prestressing steel" Proceedings 3rd. FIP Symposium, FIP-Berkeley, Wexham Springs. Slough U.K., 1981.
- (3) Sánchez-Gálvez, V., Elices, M., "On hydrogen induced cracking in prestressing steel wires". Proceedings of the 5th European Conference on Fracture (ECF5). Edited by L. Faria, Lisboa. Portugal. 1984, pp.1003-1014.
- (4) Elices, M., Maeder, G., Sánchez-Gálvez, V., British Corrosion Journal, Vol.18, No.2, 1983, pp.80-81.
- (5) Toribio, J., "Fractura elastoplástica de alambres entallados". Ph. D. Thesis Doctoral, Polytechnical University of Madrid, 1987.
- (6) Toribio, J., Elices, M., "Role of diffusion in the hydrogen transport in metals", ECF8, 1990.
- (7) Van Leeuwen, H.P., Engng. Fracture Mech., Vol.6, 1974, pp. 141-161.
- (8) Astiz, M.A., "Hydrogen diffusion analysis in metals" in " Computational Methods for Non Linear Problems". Edited by C. Taylor, B.R., Owen and E. Hinton, Pineridge Press, 1987, pp. 271-299.
- (9) Crank, J., "The Mathematics of Diffusion", Oxford University Press, 1975.
- (10) Piñero, J.M., "Tenacidad de fractura de alambres frente a la fragilización por hidrógeno". Ph.D. Thesis, Polytechnical University of Madrid, 1981.
- (11) Astiz, M.A., Int. J. Fract., Vol.31, 1986, pp. 105-124.

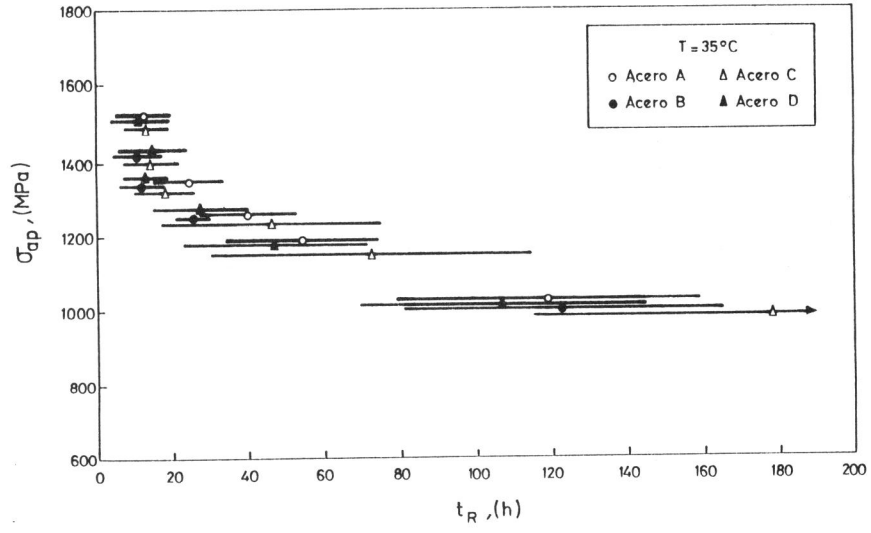


Fig.1. Experimental results of the FIP test

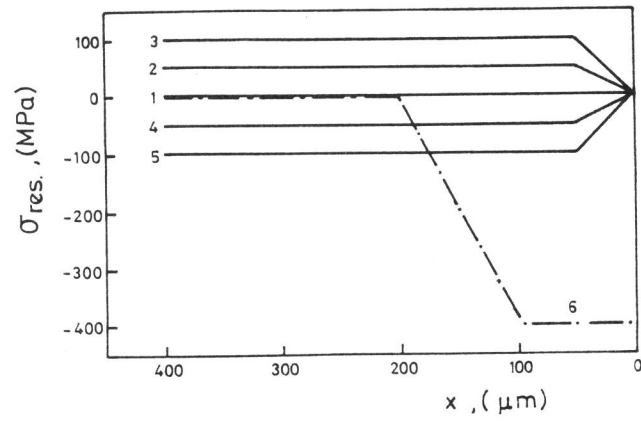


Fig.2. Residual stress distributions



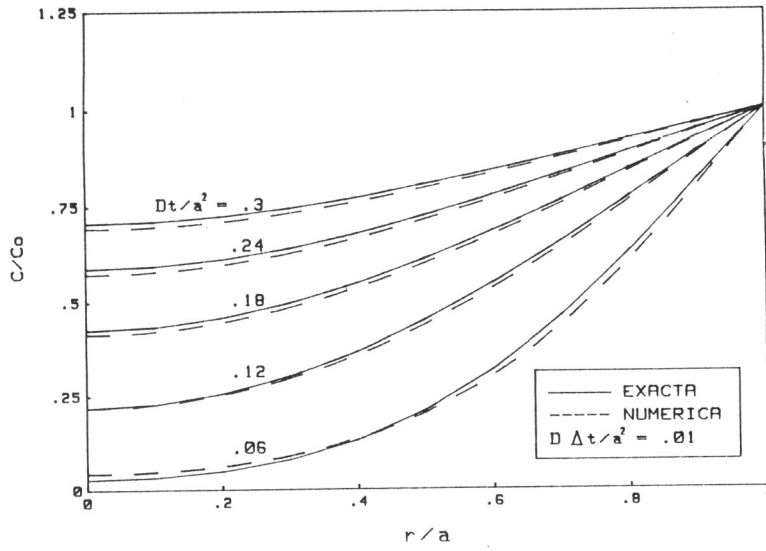


Fig.3. Exact and numerical solutions for the diffusion in a cylinder without stresses

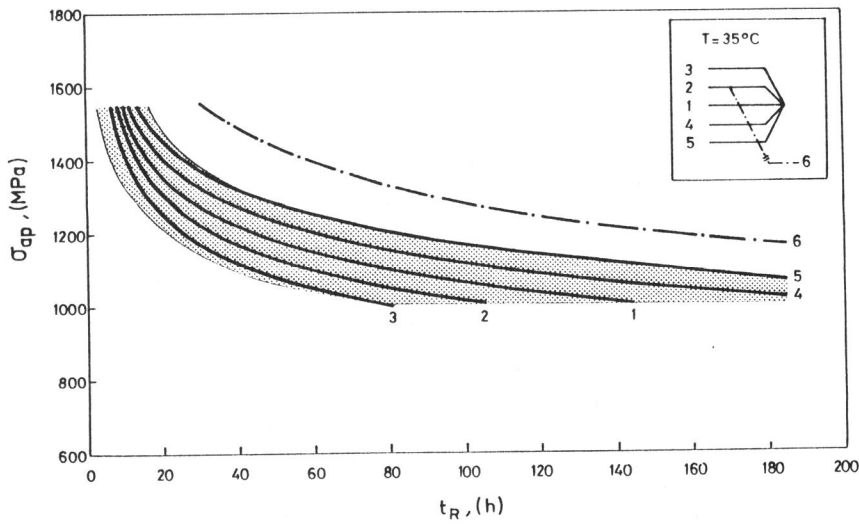


Fig.4. Comparison between theoretical model and experimental results (shaded area).